

Smithsonian Astrophysical Observatory Laser Tracking Systems [and Discussion]

M. R. Pearlman, N. W. Lanham, C. G. Lehr, J. Wohn and J. A. Weightman

Phil. Trans. R. Soc. Lond. A 1977 **284**, 431-442

doi: 10.1098/rsta.1977.0016

Email alerting service

Receive free email alerts when new articles cite this article - sign up in the box at the top right-hand corner of the article or click [here](#)

Smithsonian Astrophysical Observatory laser tracking systems

BY M. R. PEARLMAN, N. W. LANHAM, C. G. LEHR AND J. WOHN

Smithsonian Astrophysical Observatory, Cambridge, Massachusetts 02138, U.S.A.

The Smithsonian Astrophysical Observatory operates four laser satellite-ranging systems in support of geodetic and geophysical research. The lasers—located in Brazil, Peru, Australia, and Arizona—have been in operation for more than 5 years and have provided ranging data at accuracy levels of a metre or better. To meet new requirements in geophysics, these systems are now being upgraded to improve range accuracy and performance.

The lasers are being equipped with electronic pulse processors, to analyse return-pulse wave shape, and pulse choppers, to reduce laser pulse width. Initial results indicate that the upgraded ranging system hardware will meet the decimetre ranging-accuracy requirements for the Geos 3 and Seasat satellites and for Earth-dynamics projects based on satellites such as Starlette.

1. INTRODUCTION

Over the past several years, geodetic satellite techniques have begun to play an important role in geophysical research programs. Geos 3, with its on-board radar altimeter, has been mapping ocean-surface topography to submetre accuracies in support of investigations in both solid-Earth physics and oceanography. Seasat, planned for launch in 1978, will perform ocean-surface altimetry to an accuracy of 10 cm. Starlette, currently in orbit, and Lageos, scheduled for launch in 1976 (successfully launched on 4 May 1976), are cornerstones in the development of future geodetic models for the gravity field and station positions and are intended to support research of dynamic geophysical phenomena. These and other related satellite programs require very accurate orbit determination, either as a means of data interpretation, as with the altimeter, or as a direct measure of desirable quantities, as in the development of gravity-field models. These programs are relying on laser ranging to provide high-accuracy tracking data.

The Smithsonian Astrophysical Observatory (S.A.O.) operates four satellite-ranging laser systems to support research in geodesy and geophysics. The S.A.O. systems, which have been in routine operation for more than 5 years, are located in Natal, Brazil; Arequipa, Peru; Orroral Valley, Australia; and Mt Hopkins, Arizona. These systems were originally deployed at Baker–Nunn stations that complemented existing or planned laser sites by other active groups. Three were placed in the Southern Hemisphere to enhance global coverage. One of those three, originally located in Olifantsfontein, South Africa, is now being moved to Australia. These, and similar laser ranging systems operated in close coordination by other groups around the world, have provided the fundamental tracking and network support for many research programmes.

Originally designed for the needs of the Observatory's programme in satellite geodesy, the S.A.O. lasers are now being upgraded in performance and in accuracy to meet new geophysical requirements. During the last year, the S.A.O. laser systems have been equipped with pulse-processing electronics to overcome systematic and random range errors due to variations in laser output and return waveforms. Now work is under way to provide the systems with pulse choppers to reduce the laser pulse width. We anticipate that the system hardware will have 10 cm ranging accuracy to near-Earth satellites when the current upgrading programme is completed in 1976.

2. HARDWARE

The S.A.O. laser ranging system, shown in figures 1 and 2, has a static-pointing mount (or pedestal) aimed by means of computed predictions of satellite azimuth and altitude. This method of steering permits the system to operate during the day as well as at night. A static-pointing mount was selected because it is economical and operationally simple and can be maintained at remote locations.

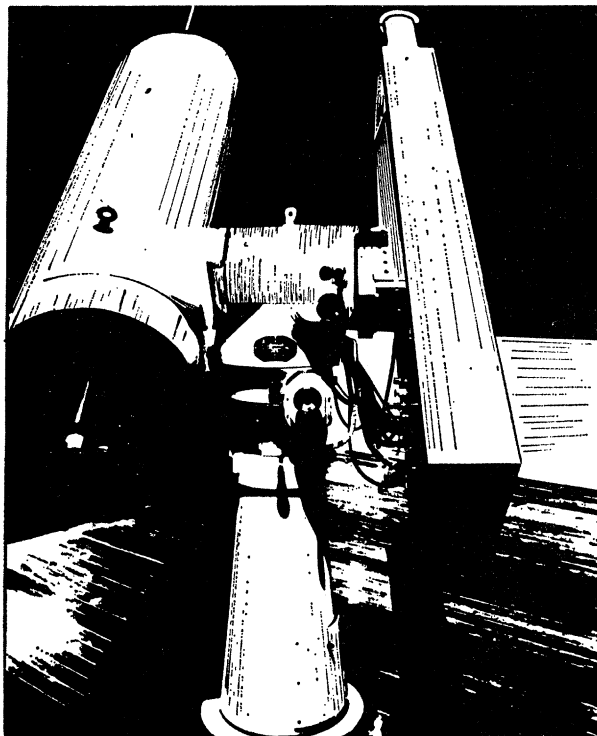


FIGURE 1. View of the S.A.O. laser tracking system.

(a) *Laser transmitter*

The laser, a ruby system built in an oscillator-amplifier configuration, generates an output of 5–7 J in a 25 ns pulse (half-power, full width). The system uses a Pockels cell and a Brewster stack for a Q -switch and operates at 8 pulses per minute. Both the 0.95 cm ($\frac{3}{8}$ in) diameter oscillator ruby rod and the 1.6 cm ($\frac{5}{8}$ in) diameter amplifier ruby rod are mounted in 15.2 cm (6 in) double elliptical cavities, each containing two linear flashlamps. The optical cavity of the oscillator is formed by a flat rear mirror, with a reflectivity of 99.9%, and the uncoated front of the oscillator rod.

The oscillator output of 1–2 J is coupled into the amplifier through a beam-expanding telescope. The amplifier has a single-pass gain of about 5. Both ends of the amplifier rod are antireflective-coated. The amplifier output is expanded to a diameter of 7 cm and passes through the 12.7 cm (5 in) objective lens of a Galilean telescope. The diameter of the output-beam divergence can be adjusted from 0.5 to 5.0 mrad. Mounted at the output of the laser, photodiodes pick up atmospherically scattered light from the outgoing pulse and send an electrical start signal to the ranging-system electronics. Additional details on these lasers are given in Pearlman *et al.* (1973).

To meet upcoming requirements, the S.A.O. lasers are being equipped with a pulse chopper to improve accuracy. The first unit has undergone testing at Mt Hopkins and has been returned to the vendor for some modifications. The chopper has been designed to fit between the present laser oscillator and amplifier sections, thus simplifying installation in the field.

The chopper is a spark-gap-activated Pockels cell, with appropriate polarizers providing the necessary transmission and isolation. Isolation is required in this configuration to prevent depletion of the amplifier's upper energy level. The polarizers are commercially available dielectric-coated plates mounted at the Brewster angle. The chopper also uses a quartz half-wave plate in the transmission path to rotate the optical polarization and to permit the Pockels cell to operate in the voltage-on transmission mode. The output pulse width is adjustable, but the laser is expected to produce 0.5 J at a pulse width of 6 to 7 ns.

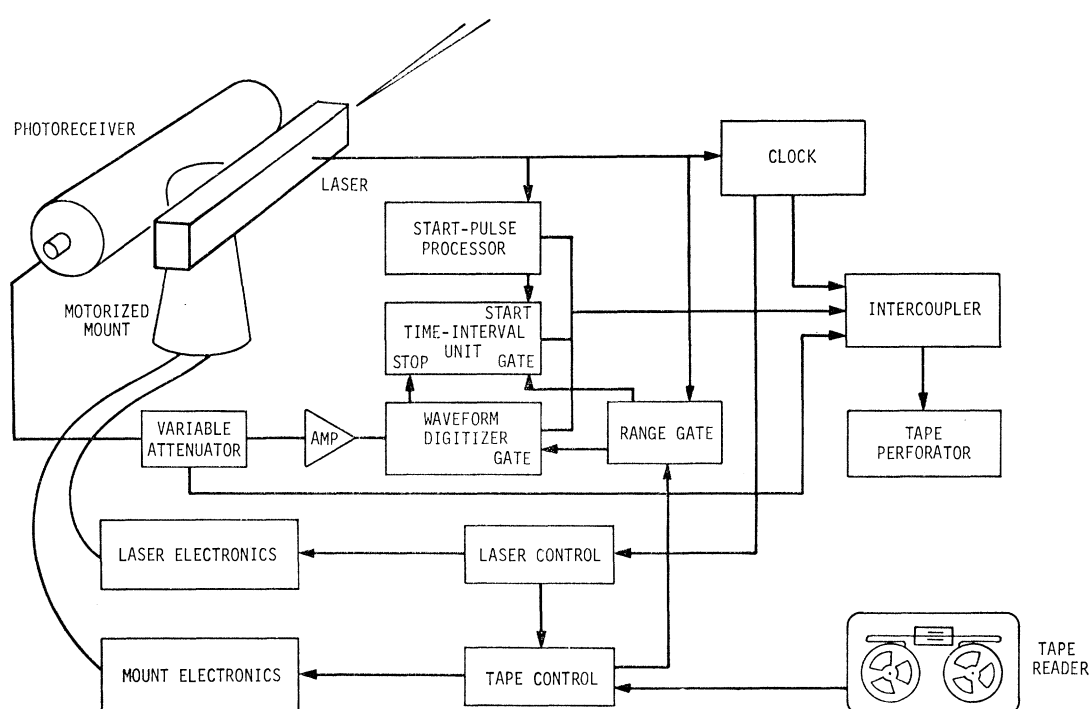


FIGURE 2. Block diagram of the laser system.

(b) *Ranging-system electronics*

The ranging-system electronics consist of a clock, a firing control, a range-gate control, a processing system for the start and stop (return) pulses, a time-interval unit, and a data-handling system (intercoupler) (see figure 2). The clock, synchronized to within $\pm 1 \mu\text{s}$ of each station's master clock, controls the firing time of the laser and provides the epoch of observation. Both the firing rate and the time of the laser firing are controlled by the laser control unit. The firing time can be shifted manually by multiples of 0.001 s, with a maximum of ± 3 s, to account for the early or late arrival of a satellite at a predicted point in its orbit. The range-gate control unit provides a delayed pulse of adjustable width to gate the counter and the pulse-processing system. This range gate protects against triggering by sky background or electronic noise. The time-interval unit, which has a resolution of 0.1 ns, is triggered on and off by outputs from the pulse-processing system.

A pulse-processing system has been used in the S.A.O. lasers to minimize range errors due to irregularities in the wave shape. The system permits us to produce range measurements referred to pulse centres rather than to fixed- or variable-threshold points. This substantially reduces both the random and the systematic errors introduced, with threshold-detection techniques, by irregularities in return-pulse size and shape and by changes in the laser output energy and pulse width. With fixed-threshold systems, these errors can be comparable in size to the laser output pulse width (Lehr, Pearlman & Scott 1970).

The pulse processor is divided into two sections, the start and stop channels. The laser output pulse is sampled by the start channel, which produces a threshold-activated pulse of constant size and shape that starts the time-interval unit. The start channel also supplies d.c. signal levels, which are measurements of the transmitted pulse width (at a preset threshold level) and area (energy). The stop channel digitizes the return-pulse waveform and provides a pulse of fixed size and shape that stops the time-interval unit. This stop pulse is synchronized to a time reference point on the waveform. During data preprocessing, the transmitted and return-pulse information furnished by both channels is used to extrapolate range measurements to pulse centres.

The start channel is based on dual discriminators and pulse integrators. The pulse data are digitized and fed to the data intercoupler, in b.c.d. format. The stop channel is centred around a commercially available waveform digitizer, which provides a visual and b.c.d. display of the return pulse. The digitizer has 20 sampling channels with spacing adjustable in steps from 1 to 25 ns.

The laser data system furnishes all the data, plus housekeeping and support information, which are produced on punched paper tape for subsequent processing.

(c) *Mount*

The azimuth-altitude static-pointing mount has a pointing accuracy of better than $\pm 30''$. The system is driven by stepping motors in an open-loop mode, with the stepping-motor drive-system gears allowing for slewing speeds of 2° s^{-1} and positioning increments of 0.001° . The mount has goniometers graduated to 0.001° for reference and verification. Predictions, including pointing angles and range-gate settings, are entered in the system on a point-by-point real-time basis.

(d) *Photoreceiver*

The receiving telescope is a 50.8 cm (20 in) Cassegrain system with additional optics designed to focus an image of the primary mirror on the photocathode of the photomultiplier tube. The optics following the flat secondary mirror passes the collimated return signal through a 0.7 nm filter that is both tilt- and temperature-dependent. Effects of age and temperature are compensated for by means of a micrometer tilt adjustment that tunes the filter. Adjustable field stops and a provision to insert combinations of neutral-density filters are available.

The photodetector, an RCA 7265, was chosen for its quantum efficiency of 4% at 694.3 nm. The p.m.t. has a gain of 5×10^7 and a risetime of approximately 3 ns as operated in the S.A.O. system.

(e) *Minicomputer*

The S.A.O. laser stations have been equipped with minicomputers for generating pointing predictions from orbital elements and for preprocessing calibration and satellite-ranging data. The system is now operated in a stand-alone mode. Our long-range plan is to connect the minicomputer directly to the ranging system.

Each minicomputer has 16 384 words of 16-bit core memory and a floating-point processor. Its peripherals include three block-addressable magnetic-tape units, an alphanumeric c.r.t. display unit, a high-speed paper-tape reader and punch, and a console teletypewriter.

(f) *Station timing*

All the stations have a timekeeping system to provide precise epoch for each observation and a stable reference source for time-interval measurements. The clocks consist of rubidium oscillators, a time accumulator, and a system of time and frequency monitoring aids. The clocks have dual-channel redundancy and a battery-backed power system to guard against loss of time continuity.

The frequency of the station oscillators is maintained through frequency and phase comparisons with v.l.f. transmissions. Epoch checks are made at the stations through a combination of Loran, portable-clock trips, and local time references.

With careful analysis of the v.l.f. phase data and periodic epoch checks, we are able to maintain station timing to within 10 to 20 μ s of UTC (United States Naval Observatory).

Procurement is now under way for Timation 3 receivers for the laser stations, which should provide timing accuracies of 1 μ s on a recoverable basis.

3. SOFTWARE

(a) *Prediction program*

The laser stations use a minicomputer program to generate pointing predictions. The program, which is essentially an outgrowth of our software used in Cambridge, generates pointing angles and range-gate settings directly from orbital elements and long-period-perturbation terms. The program calculates Sun and zenith evasions for normal operation; it also has a facility to apply angle corrections to compensate for mount pointing errors.

The program was originally written in a combination of Fortran and Forth computer languages. This was undertaken because of existing Fortran routines and the relative ease of program development utilizing Forth in a nondisk-based hardware environment. A newer version is now being written entirely in Fortran.

(b) *Calibration programs*

Laser ranging systems require detailed calibration procedures to ensure system accuracy and performance (see § 4). The stations have minicomputer software to analyse both electronic and target-ranging calibration data and to diagnose operational and hardware problems.

(c) *Data-handling and quick-look programs*

Satellite-ranging data are transferred from paper tape to magnetic tape by the minicomputer system for shipment to Cambridge. The program that handles the data transfer provides a facility to examine the data on site and to generate an abbreviated quick-look data message for transmission to Cambridge to maintain prediction orbits.

4. CALIBRATION

(a) *Start-channel calibration*

The calibration of the start channel is developed as a system delay, expressed by a linear relation involving pulse width and area. Calibration is performed electronically by entering pulses of varying amplitudes and widths into both the start and the stop channels.

Start-channel calibrations show changes of a few tenths of a nanosecond or less over periods of many weeks, indicating good long-term stability for the electronics system.

(b) *Extended target calibrations*

Target calibration is used extensively in the S.A.O. operating procedures to measure system delay and to verify system stability.

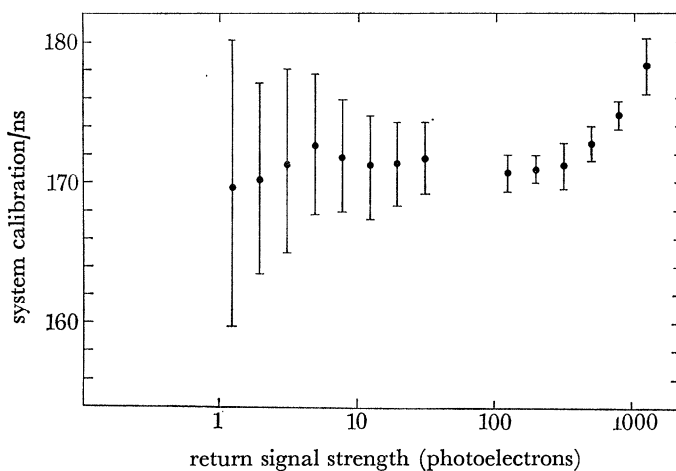


FIGURE 3. Detailed system calibration at Mt Hopkins, 18 April, 1975. Error bars denote the standard deviation of all the data in the signal-strength interval.

Detailed target calibrations over the full dynamic range of the system (one to several thousand photoelectrons) have shown that the system calibration can depend on return-signal strength under some conditions. The dependence appears as an increase of a few nanoseconds in the calibration constant at high signal levels. A typical example based on 2000 measurements is presented in figure 3. Through nearly a year of operation at Mt Hopkins, with many changes in system configuration resulting in shifts of the overall calibration level, the general shape of the calibration curve has not changed appreciably. The signal-strength dependence appears to be from saturation within the photomultiplier, which results in asymmetrical pulse broadening at the digitizer. The apparent structure at low signal strength is probably due to insufficient sampling at the lower level signals. The system-calibration curve varies from one photomultiplier to another; in some cases, no dependence on signal strength is apparent. Decreasing the photomultiplier gain by reducing the applied voltage also reduces the signal-strength dependence.

Once system stability has been verified, extended target calibrations are taken weekly. For processing satellite observations, S.A.O. is currently using a piecewise linear model for system calibration when the signal-strength dependence is present. A typical model, based on 7000 data points taken over a period of several months, assumes a constant system delay for signal strengths up to several hundred photoelectrons and then a straight-line fit to the data above that value.

(c) Pre-pass and post-pass target calibrations

In addition to the signal-strength dependence, variations in system configurations will shift the system calibration curve up or down from time to time. Changes in cables, components, subsystems and subsystem calibrations affect overall system calibration.

In satellite-ranging operations, target calibrations of 25 pulses each are performed before and after each satellite pass. The precalibrations and postcalibrations, which are performed at a prescribed reference signal strength (about 100 photoelectrons), are submitted to processing along with the satellite range data. The system calibration relation (determined by the extended target-calibration analysis) is normalized on a pass-by-pass basis from the mean value of the two calibration runs. The difference in the values of the pre-calibrations and post-calibrations is used to estimate the short-term system stability during a satellite pass; this difference is stored with the data for reference during analysis.

5. STATION OPERATIONS

The S.A.O. stations are operated on a routine daily basis to support Observatory programs. Each station has approximately six individuals devoted to laser operations; they usually maintain operation for at least 80–100 h a week. These hours are shifted when necessary to provide coverage for high-priority passes.

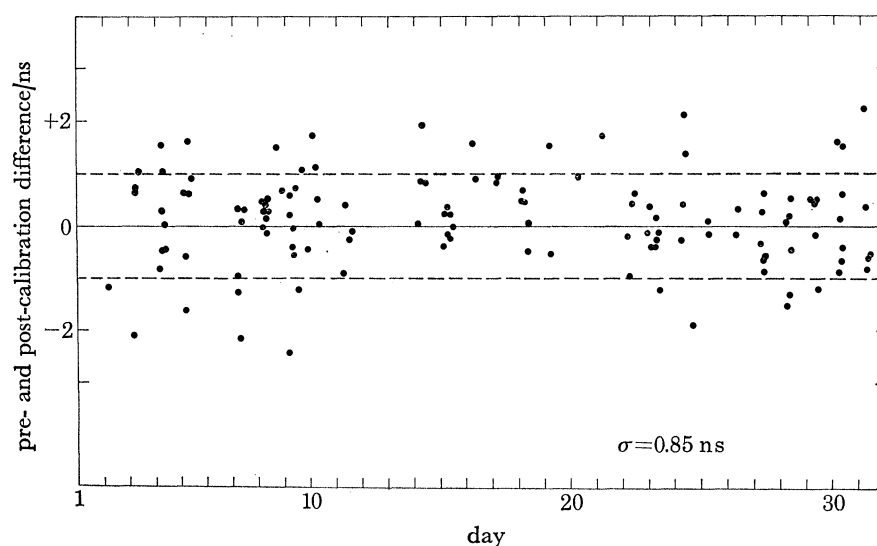


FIGURE 4. Calibration stability of the Mt Hopkins laser: pre-calibration minus post-calibration, October 1975.

6. SYSTEM PERFORMANCE

System performance has been examined through analysis of target-calibration and satellite-ranging data. Although the upgrading is at an interim stage, the implementation of the pulse processor has already had an effect on the range data. The installation of the pulse chopper is expected to produce an additional improvement in range accuracy.

(a) System stability

The short-term system stability can be estimated from the difference between pre-pass and post-pass target calibrations.

Data taken during the last year at Mt Hopkins and during the last 6 months in Natal show this calibration difference to have a standard deviation of about 1.0 ns. Sample data are shown in figure 4. These data contain measurement errors due to the 25 ns pulse width, to the finite number of data points in each calibration measurement, and to the sampling spacing (5 or 10 ns) of the waveform digitizer. The uncertainty associated with each pre- and post-calibration set from pulse and sampling considerations may be the dominant source of data scatter in figure 4. With a narrow laser pulse, we expect to obtain better estimates of system stability.

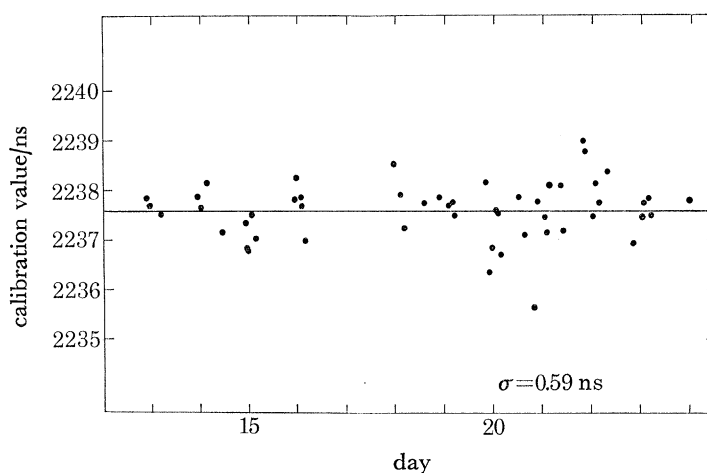


FIGURE 5. Mean target calibration data from the Natal, Brazil, laser, September 1975.

The long-term system stability can be examined from a sequence of average values of the pre-pass and post-pass target calibrations. Target-calibration data from Natal (figure 5) show that variations in system calibration are typically 1 ns over periods when the hardware configuration is not changed. Once again, pulse width and sampling spacing probably account for a significant part of the scatter.

(b) Range noise

At low signal strength the random error due to photon quantization at the photomultiplier dominates other noise sources in the system. This is apparent from the extended target-calibration data (see figure 3). At higher signal strengths, the noise appears to reach a lower limit of 0.4–1.6 ns for the systems tested. This is probably due to jitter in the photomultiplier and to the large sampling intervals used with the wide laser pulse.

Range noise in satellite data is a combination of random photon quantization effects, laser wavefront distortion (Billiris, Papagiannis, Lehr & Pearlman 1975), detection-system jitter and sampling, propagation effects, and satellite characteristics. Typical satellite passes with the 25 ns laser pulse have standard deviations from polynomial approximations to short-arc fits of 20–40 cm. An example is shown in figure 6. Return-signal strengths can vary from a few photoelectrons to almost 1000 during a pass; however, the preponderance of data are in the range of 20–200 photoelectrons.

(c) System accuracy

Ranging errors are introduced by the system from three sources: the laser transmitter, the detection system, and calibration. We restrict ourselves here to the ranging-system hardware and leave other areas, such as refraction, timing, and spacecraft retroreflector-array characteristics, for discussion elsewhere.

In its present wide-pulse operating mode, the laser transmitter may introduce range errors due to wavefront distortion. Experiments conducted at Mt Hopkins showed that the wavefront had a structure amounting to several nanoseconds across the laser beam and that the structure was impossible to forecast or model effectively through calibration techniques. Root-mean-square variations in the time of arrival across the beam were typically 0.6–1.6 ns (Billiris *et al.* 1975).

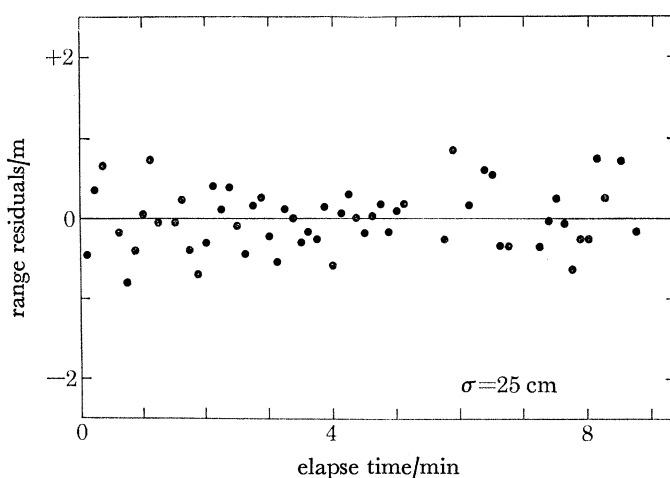


FIGURE 6. Range residuals to a short-arc orbital fit on Geos 2 from the Natal, Brazil, laser (3 November 1975, 4 h 8 min U.T.).

From the results of the extended target calibrations (see figure 3), we can estimate the error introduced by the detection system. At high signal strengths (~ 1000 photoelectrons), the random error due to quantization is small and the range error, which is typically 1 ns or less, can be attributed to detection-system performance (see § 6*b*).

Ranging errors are introduced into the data through uncertainties in the system calibration characteristics and through calibration normalization. In some cases, the extended target ranging data used to develop system calibration characteristics show system-delay variations over much of the range in signal strength (see figure 7). It is not clear if all this structure is real, nor has a fully satisfactory explanation for it been found. Rather than fitting a fictitious curve to the data, we use the piecewise linear model (discussed in § 4*b*) based on long-term averages of the extended calibration data. This seems more plausible physically, but in recognition of variations in the data, we ascribe an uncertainty to the calibration characteristics. For this uncertainty, we choose a standard deviation about the linear model for the high-density, well-defined data points (shown in figure 7), which are usually less than 1 ns but may be as large as 1.6 ns for some cases.

Calibration normalization is developed on a pass-by-pass basis through pre-pass and post-pass calibrations (see § 4*c*). The error introduced by this procedure can be estimated by the observed standard deviation for the pre- and post-calibration differences. This value is typically 1 ns.

Each of the major sources of error – wavefront distortion, photoreceiver and detection system, calibration characteristics, and calibration normalization – introduces a range error of about 1 ns at high signal strengths. At lower signal levels, the larger errors, due to photon quantization introduced by the photoreceiver and the detection system, are random, and averaging over a satellite pass should reduce their influence to the 1 ns error found at high signal strengths. Since these major sources of error are uncorrelated, the total system accuracy is about 2 ns.

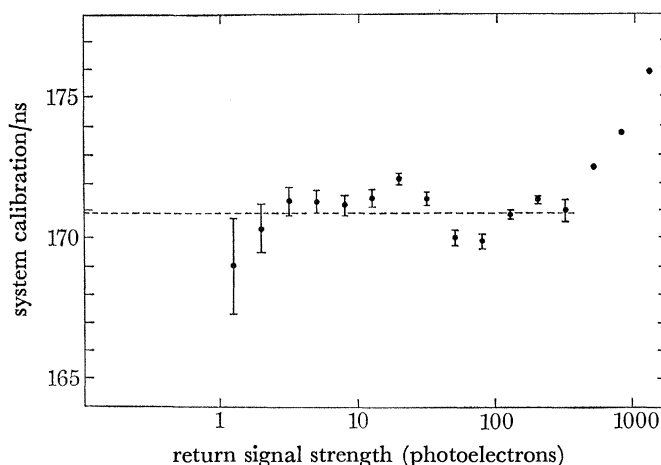


FIGURE 7. System calibration at Mt Hopkins, long-term average. Standard deviation (flat segment) = 0.83 ns. Error bars denote the estimate of the mean of all the data in the signal-strength interval.

The implementation of the pulse chopper is expected to reduce uncertainties in all four areas. The chopper will regulate the final emission times for all the laser modes and should, therefore, alleviate the wavefront problem. The reduction in pulse width will decrease the random error due to photoquantization, particularly at low and intermediate signal strengths; it will also permit finer sampling-channel spacing to be used with the waveform digitizer, which may improve system noise in the high-signal-strength region. For similar reasons, the narrow-pulse operation should reduce the error in calibration normalization and should give better definition of the calibration characteristics from detailed target ranging.

TABLE 1. SATELLITE PASSES (APRIL 1975–JANUARY 1976)

station	BE-C	Geos 1	Geos 2	Starlette	Geos 3	total
South Africa (7 months)	3	314	271	301	223	1112
Peru (9 months)	439	442	386	433	335	2035
Arizona (6 months)	155	167	91	133	127	673
Brazil (7 months)	167	208	168	185	124	852
totals	764	1131	916	1052	809	4672

(d) *Data yield*

Since April 1975, the S.A.O. network has been involved in the Geos 3 tracking program. Field operations have focused on tracking support for Geos 3 (particularly on high-priority orbits during altimeter operations) and on routine tracking of several other satellites for a general

revision of the gravity-field and station-position models. The data yield for the network during this period is shown in table 1, along with the number of months of operation.

All the stations have been in operation for a significant portion of the campaign period, although all but Peru and Greece were closed for 2 or 3 months for station upgrading.

At the four S.A.O. stations, satellite passes generally contain 30–60 data points; cases of 120–150 occur when orbital geometry and local conditions are favourable. In clear skies, the lasers are able to get returns as close as 10° to the horizon from Geos 3 and Starlette, which were designed for low-zenith-angle coverage.



FIGURE 8. S.A.O. laser tracking network.

7. S.A.O. LASER NETWORK AND INTERNATIONAL COOPERATION

The S.A.O. laser tracking network (see figure 8) consists for the four S.A.O. lasers plus lasers operated by cooperating agencies in Athens (National Technical University) and Tokyo (Tokyo Astronomical Observatory). In addition to a long-standing relationship with the laser tracking activities of the National Aeronautics and Space Administration, S.A.O. also has maintained very close coordination with laser tracking groups at the Centre National d'Etudes Spatiales, France; Institut für Angewandte Geodäsie, West Germany; and Technische Hogeschool Delft, Netherlands. S.A.O. routinely supplies these groups with orbital elements for pointing predictions and accepts quick-look data for orbital maintenance. In some cases, S.A.O. provides operational, scheduling, data-screening, and technical and personnel support.

This work was supported in part by National Aeronautics and Space Administration Grant NGR-09-015-002.

REFERENCES (Pearlman *et al.*)

- Billiris, H. G., Papagiannis, M. D., Lehr, C. G. & Pearlman, M. R. 1975 Beam wavefront distortions in a laser ranging system. *Smithsonian Astrophys. Obs. Laser Rep.* no. 7, 19 pp.
- Lehr, C. G., Pearlman, M. R. & Scott, J. L. 1970 Range corrections from oscilloscopic displays of laser returns. *Smithsonian Astrophys. Obs. Laser Rep.* no. 4, 27 pp.
- Pearlman, M. R., Thorp, J. M., Tsiang, C. R. H., Arnold, D. A., Lehr, C. G. & Wohn, J. 1973 SAO network: Instrumentation and data reduction. In *1973 Smithsonian Standard Earth (III)* (ed. E. M. Gaposchkin). *Smithsonian Astrophys. Obs. Spec. Rep.* no. 353, pp. 17–84.

Discussion

J. A. WEIGHTMAN (*Geodetic Office, Elmwood Avenue, Feltham, Middlesex*). While global map projections are notoriously misleading, the graphic showing the four main S.A.O. satellite laser stations (Mount Hopkins, Arequipa, Natal and Orroral Valley) suggests that they are roughly coplanar in position. Was this intentional and are there benefits to offset any instability from ill-conditioned geometry of observations based on these?

M. R. PEARLMAN. The S.A.O. stations are not co-planar, nor were they intended to be. With our methods of analysis, it would not make any difference if the stations were co-planar.